Electronic Supplementary Material (ESI) for Catalysis Science & Technology.

Supporting information

for

Maximizing *n*-Alkane Hydroisomerization: The Interplay of Phase, Feed Complexity and Zeolite Catalyst Mixing

Bart D. Vandegehuchte, Joris W. Thybaut, Johan A. Martens, and Guy B. Marin

Table of Contents

The supporting information accompanying the manuscript 'Exploring the Synergy between Zeolites Exhibiting Complementary Confinement Behavior in Ideal *n*-Alkane Hydroconversion' provides a concise overview of the modeling methodology adopted to simulate *n*-alkane hydroconversion reactions in an ideal plug flow reactor. The fundamental kinetic model forms the core of the present methodology, and is based upon the single-event concept specifically designed to cope with large, complex reaction networks. The prominent literature regarding this matter is referred to in this text in order to direct the reader to more detailed elaborations if this would be required.

1 Reactor model development

An isothermal, pseudohomogeneous one-dimensional plug flow reactor model was applied as follows for, e.g., reaction product *i*:

$$\frac{dF_i}{dW} = R_i \tag{1}$$

Herein, F_i represents the molar flow rate of component *i*, R_i its net production rate, and *W* the catalyst mass. The molar outlet flow rate of each reaction product was determined by integrating the corresponding set of ordinary differential equations. To this purpose, the DVODE subroutine available at NETLIB [1], was incorporated in an in-house written FORTRAN code. The flow rate of the primary feed component and hydrogen were calculated a posteriori from the atomic carbon and hydrogen balance, respectively. The feed conversion is defined as:

$$X_{tot} = \frac{F_{feed}^{\ 0} - F_{feed}}{F_{feed}^{\ 0}} \tag{2}$$

In case of a feed mixture, the conversion of a single feed component *i* is defined as:

$$X_i = \frac{F_i^0 - F_i}{F_i^0} \tag{3}$$

Upon feeding a mixture one of the feed components might be formed out of another one. In the present work for parapur hydroconversion, (s;s) β-scission of a tridecyl isomer carbenium ion could result in the formation of a decyl ion or a decene. As this reaction contributes only slightly to the overall reaction scheme, Eqn. 2 remains an accurate formula for calculating the total parapur conversion. The yield towards a product *i* is defined as:

$$Y_i = \frac{F_i}{F_{feed}^{\ 0}} \tag{4}$$

In case of a feed mixture, the yield is expressed with respect to the corresponding *n*-alkane in the denominator of Eqn. 4. The total isomerization yield is defined as the sum over all individual isomer yields:

$$Y_{iso} = \sum_{i=1}^{niso} Y_i \tag{5}$$

2 SEMK model for gas-phase alkane hydroconversion on non-shape selective catalysts

A single catalytic cycle in alkane hydroconversion comprises consecutive dehydrogenation and protonation on respectively metal and acid sites, followed by acid-catalyzed cracking and isomerization [2-4]. The acid-catalyzed reactions primarily comprise β-scission, alkyl shift and branching over a Protonated CycloPropane (PCP) transition state, and are generally rate-determining. The latter implies quasi-equilibration of the dehydrogenation reactions towards alkenes, which is equivalent with 'ideal hydroconversion' [5-7], and of the protonation reactions towards carbenium ion intermediates. Upon their entry in the catalyst micropores, sorbate alkanes experience physical Van der Waals forces exhibited by the catalyst framework. The physisorption equilibrium is quantified by means of a Langmuir isotherm, e.g., for component *i*:

$$C_i = \frac{C_i^s K_i^L p_i}{1 + \sum_{u=1}^{npar} K_u^L p_u} \tag{6}$$

Herein, the Langmuir physisorption coefficient comprises the standard physisorption enthalpy and entropy:

$$K_i^L = 0.5 p^{0-1} e^{\frac{\Delta S_i^{0,phy}}{R}} e^{\frac{-\Delta H_i^{0,phy}}{RT}} \tag{7}$$

Assuming equilibration for (de)hydrogenation and (de)protonation, the following expression is obtained for the rate of an acid-catalyzed isomerization or cracking step [8]:

$$r_{k,l} = k_{k,l} \frac{C_i^s C^{acid} K_i^L K_{i,j}^{deh} K_{j,k}^{pro} p_i p_{H_2}^{-1}}{1 + \sum_{u=1}^{npar} K_u^L p_u + \sum_{u=1}^{npar} \sum_{v=1}^{nole} C_u^s K_u^L K_{u,v}^{deh} K_{v,w}^{pro} p_u p_{H_2}^{-1}} \tag{8}$$

The symbols are explained in the Nomenclature (Section 6). The reactant carbenium ion is denoted as *k* and is formed from alkene *j* via protonation which, in turn, originates from the dehydrogenation of alkane *i*. The catalyst descriptors in Eqn. 8 are the physisorption saturation concentration, the total acid site concentration, the Langmuir physisorption coefficient, and the protonation equilibrium coefficient. The standard protonation enthalpy depends only on the type of product ion formed, and was found to be an accurate descriptor for the average acid strength of the catalyst [2, 3]. The net production rate of each alkane is calculating by assuming pseudo steady-state for the alkene and carbenium ion intermediates.

The SEMK methodology enables to relate the rate coefficient $k_{k,l}$ to an intrinsic, single-event rate coefficient $\tilde{k}$ reflecting the actual chemistry involved. The latter is unique for the reaction family to which the elementary step belongs. Reaction families are introduced based upon the elementary step type, and the reactant and product carbenium ion type. Doing so, and accounting for thermodynamic consistency, a limited number of 10 single-event rate coefficients are to be determined for alkane hydroconversion [8, 9], which are catalyst independent according to the free carbenium ion chemistry that has been assumed [2]. Differences between the single-event and the actual rate coefficient of an elementary step stem from symmetry and chirality effects which are assessed by the so-called 'number of single events', n_e, which quantifies the number of structurally equivalent ways in which the elementary step can occur [10]. It is concordantly calculated from the global symmetry numbers of reactant and transition state:

$$n_e = \frac{\sigma_{glob,R^+}}{\sigma_{glob,\neq}} \tag{9}$$

Doing so, the actual rate coefficient is expressed as follows:

$$k_{k,l} = n_e \tilde{k}(m_k;m_l) \tag{10}$$

with m_k and m_l the types of carbenium ions *k* and *l*. The global symmetry numbers and, consequently, the numbers of single events of all elementary steps are automatically generated, together with the reaction network, by means of an in-house written network generation program based upon Boolean matrix representations [11].

3 Phase effects during liquid-phase reaction

SEMK modelling of *n*-alkane hydroconversion at liquid phase conditions was intensively elaborated by Marin and co-workers using a non-shape selective Pt/H-USY [12, 13], as well as a shape selective

Pt/H-ZSM22 [14]. Essentially, deviations from the ideal gas state during physisorption need to be accounted for by liquid phase fugacity coefficients, while destabilization of the sorbate molecules caused by intermolecular compression effects were accounted for by the excess free enthalpy of physisorption [15, 16]:

$$\Delta G_i^{0,phy,l} = -RT\ln\phi_i^L + \Delta G_i^{0,phy,g} + \Delta G_i^{0,phy,E} \qquad (11)$$

The extent of sorbate compression is affected by the 'flexibility' of the sorbent framework which adapts itself to the physisorbed phase to attain a minimum free enthalpy configuration [17, 18]. Eqn. 11 follows from a Born-Haber cycle in which physisorption from the liquid phase is expressed as a function of (1) the liquid fugacity coefficient assessing the bulk phase non-ideality in reference to the ideal gas state, (2) the standard free enthalpy for physisorption from the ideal gas phase, and (3) the excess free enthalpy of physisorption, $\Delta G_i^{0,phy,E}$, quantifying sorbate destabilization by the surrounding physisorbed phase [13]. The latter parameter could be expressed as a function of the liquid fugacity coefficient of the species involved, and an adjustable excess parameter c^E:

$$\Delta G_i^{0,phy,E} = -c^E\ln\phi_i^L \qquad (12)$$

Implementation of Eqns. 11 and 12 into a generalized Langmuir isotherm yields a similar expression for the physisorbed alkane concentration as was obtained earlier in Eqn. 6 for reaction from the gas phase:

$$C_i = \frac{C_i^s K_i^L {\phi_i^L}^{1+\frac{c^E}{RT}} p_{tot} V_{mol,i} C_i^L}{1 + \sum_{u=1}^{npar} K_u^L {\phi_u^L}^{1+\frac{c^E}{RT}} p_{tot} V_{mol,u} C_u^L} \qquad (13)$$

Herein, the component fugacity f_i is expressed as the product of the liquid fugacity coefficient, the total pressure p_{tot}, the species concentration in the liquid phase, C_i^L, and its molar volume $V_{mol,i}$:

$$f_i^L = \phi_i^L C_i^L V_{mol,i} p_{tot} \qquad (14)$$

The liquid phase fugacity coefficient deviates more strongly from unity with increasing sorbate size, hence, implying that the destabilization effect of the physisorbed phase is more pronounced for larger molecules. Chemisorption on an active site is affected in a similar way as the physisorption step owing to compression and framework solvation. The latter was also suggested earlier from transition state theory [19]. A standard free enthalpy for protonation excess, $\Delta G_i^{0,pro,E}$, was introduced to account for these effects following a similar Born-Haber cycle [13]:

$$\Delta G_i^{0,pro,l} = \Delta G_i^{0,pro,g} + \Delta G_i^{0,pro,E} \tag{15}$$

Assuming that enthalpy effects prevail over entropy effects, and an identical variation in energy level upon protonation for any carbenium ion involved in the reaction network, only one additional enthalpy term needs to be incorporated in the protonation equilibrium coefficient. This 'excess' standard protonation enthalpy constitutes one of the two additional catalyst descriptors introduced by the present methodology, the other one being the excess c^E parameter.

4 Extreme shape selectivity in unidirectional, medium-pore zeolites

In 1D medium-pore size frameworks, alkane physisorption strongly depends on the sorbate branching degree in contrast to physisorption on non-shape selective catalysts. Narasimhan et al. [20-22] gave a detailed overview of the pore mouth and key lock catalysis involved in both alkane physisorption and carbenium ion chemistry. This section presents a concise overview of the relevant physisorption modes and reaction rules. Physisorption in the micropores exclusively occurs with linear species, while branched isomers are limited to physisorption at the pore mouths in which only a part of the sorbate molecule, i.e., a so-called 'straight end', can be stabilized inside the pore, see Figure 1, or at the external surface. The concentration of physisorbed alkanes at the pore mouth is consequently calculated from the different physisorption modes the physisorbed alkane can adopt:

$$C_i^{pm} = \frac{C^{acid,pm}\left(\sum_{m=1}^{nmod} K_{m,i}^{L,pm}\right)p_i}{1 + \sum_{j=1}^{npar}\left(\sum_{m=1}^{nmod} K_{m,j}^{L,pm}\right)p_j} \tag{16}$$

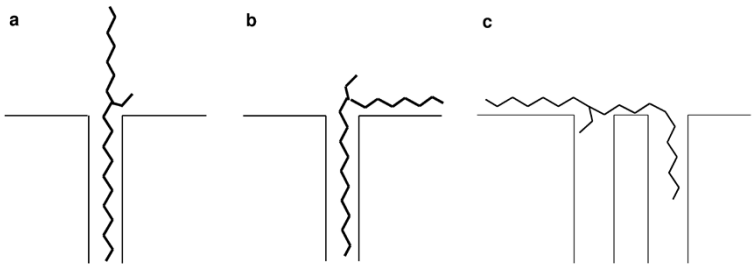

Figure 1 - Different physisorption modes of 8-ethyluncosane at a pore mouth: low interaction mode (a), high interaction mode (b), and involving two pores (c) [20].

Herein, the physisorption saturation concentration is implicitly taken equal to the total concentration of pore mouths assuming that only a single molecule can reside at a pore mouth. $K_{m,i}^{L,pm}$ represents

the Langmuir physisorption coefficient of *i* adopting mode *m* at the pore mouth. Physisorption of linear alkanes in the micropores is described according to a simple Langmuir isotherm as in Eqn. 6, introducing $K_i^{L,mp}$ as the micropore Langmuir physisorption coefficient, and with $C_i^{s,mp}$ the corresponding saturation concentration.

The standard physisorption enthalpy and entropy in Eqn. 7 for each physisorption mode is calculated from the enthalpy and entropy contribution of each carbon atom interacting with the sorbent depending on its exact position, i.e., inside the pore, outside the pore and unaligned with the framework, or outside the pore and aligned with the framework. The latter is only possible if the carbon chain dangling outside of the pore mouth is sufficiently long. The corresponding physisorption parameters were determined from model regression by Narasimhan et al. [20].

Reaction can occur at three distinct locations in the catalyst framework, i.e., in the micropores, at the pore mouths, and at bridging acid sites located at the external surface in between two pore mouths [22]. While protonation, isomerization and cracking at the bridge sites follow the unconstrained reaction network as described in Section 2, reaction at the pore mouths is significantly restricted according a number of reaction rules [21]. Tertiary carbenium ion formation is, for instance, prohibited. Isomerization and cracking reactions can only occur at the pore mouth if the charge-bearing carbon atom in the product ion can be accommodated at the pore mouth. The latter is not satisfied during alkyl shifts in which the charge position switches with the shifting side branch and, hence, obstructs the new charge-bearing carbon atom from positioning itself at the pore mouth. Reaction in the micropores solely comprises type D β-scission of a secondary carbenium ion towards a primary carbenium ion and an alkene fragment, which is subjected to a high activation energy of about 180 kJ mol^{-1} owing to the unstable nature of the product ion [21].

5 SEMK modeling of alkane hydroconversion on a catalyst mixture

Choudhury et al. [23] simulated the synergy between a Pt/NaH-Y and a Pt/H-ZSM22 catalyst by adding the alkane net production rates as calculated from the SEMK models of the individual catalysts, proportionally to their concentration in the catalyst mixture:

$$R_i = wt\%_Y R_{Y,i} + wt\%_{ZSM22} R_{ZSM22,i} \tag{17}$$

The alkane net production rates on Pt/NaH-Y were determined via the SEMK model described in Section 2 with catalyst descriptors taken from previous research [23]. The saturation concentration

was determined from the micropore volume reported herein, and the molar volume of the sorbate alkane evaluated at the reaction temperature following the Hankinson-Brobst-Thomson method [24]. The dehydrogenation equilibrium coefficient was calculated from pure component data, determined via Benson's group contribution method [25]. The standard protonation enthalpy for secondary ion formation amounted up to -54 kJ mol^{-1} only, in contrast to -72 kJ mol^{-1} for the more active Pt/H-ZSM22. The physisorption, protonation and reaction descriptors related to ZSM22 were determined by Narasimhan et al. [20-22] following the methodology described in Section 4.

Specifically for reaction from the liquid phase, a value of -3.7 kJ mol^{-1} was estimated for c^E on ZSM22 [14]. A value of -1.6 kJ mol^{-1} was determined for a USY catalyst (Si/Al = 30), which allowed to adequately describe the increased contribution to physisorption of the lighter compounds at liquid-phase conditions [13]. However, owing to its higher saturation concentration [26], a 3.4 kJ mol^{-1} more negative value for the excess parameter was required and concordantly adopted for the present Y catalyst in order to effectively simulate a similar physisorption behavior. Excess standard protonation enthalpies typically lie between -7 and -8 kJ mol^{-1} [13, 14]. A value of -7 kJ mol^{-1} was adopted for both catalysts considered. The liquid phase fugacity coefficients were calculated via the Peng-Robinson equation of state [27]. The alkane binary interaction parameters were assumed equal to zero, while those involving hydrogen were calculated via a correlation proposed by Moysan et al. [28]. The latter typically adopt values exceeding 0 owing to the pronounced solubility of hydrogen in hydrocarbons. Only one set of critical properties and one acentric factor were taken per carbon number [29].

6 Nomenclature

Roman symbols

C	concentration [mol kg^{-1}]
C^L	liquid concentration [mol m^{-3}]
c^E	physisorption excess parameter [J mol^{-1}]
F	molar flow rate [mol s^{-1}]
f	fugacity [Pa]
ΔG^0	standard free enthalpy [J mol^{-1}]
ΔH^0	standard enthalpy [J mol^{-1}]
K^{deh}	dehydrogenation equilibrium coefficient [MPa]
K^L	Langmuir physisorption coefficient [MPa^{-1}]

K^{pro}	protonation equilibrium coefficient [kg mol^{-1}]
k	rate coefficient [mol kg^{-1} s^{-1}]
$\tilde{k}$	single-event rate coefficient [mol kg^{-1} s^{-1}]
m	type of carbenium ion
n_e	number of single events [-]
$niso$	number of isomers
$nmod$	number of physisorption modes
$nole$	number of alkenes
$npar$	number of alkanes
p	partial pressure [Pa]
p^0	atmospheric pressure [Pa]
R	universal gas constant [J mol^{-1} K^{-1}]
R	net rate of production [mol kg^{-1} s^{-1}]
r	reaction rate [mol kg^{-1} s^{-1}]
ΔS^0	standard entropy [J mol^{-1} K^{-1}]
T	temperature [K]
V_{mol}	molar volume [m^3 mol^{-1}]
W	catalyst mass [kg]
wt%	mass percentage
X	conversion [-]
Y	yield [-]

Greek symbols

σ_{glob}	global symmetry number [-]
ϕ^L	liquid phase fugacity coefficient [-]

Superscripts

0	initial
acid	acid sites
E	excess
g	from the gas phase
l	from the liquid phase
mp	micropore
phy	physisorption
pm	pore mouth
pro	protonation
s	saturation

Subscripts

≠	transition state
feed	feed
i,j,k,l,u,v,w	component indices
iso	isomerization
m	mode index
R^+	reactant ion
tot	total

7 References

[1] Netlib. http://www.netlib.org.

[2] J.W. Thybaut, G.B. Marin, G.V. Baron, P.A. Jacobs, and J.A. Martens, J Catal 202 (2001) 324-339.

[3] B.D. Vandegehuchte, J.W. Thybaut, C. Detavernier, D. Deduytsche, J. Dendooven, J.A. Martens, S.P. Sree, T.I. Koranyi, and G.B. Marin, J Catal 311 (2014) 433-446.

[4] P.B. Weisz, Adv Catal 13 (1962) 137-190.

[5] J.W. Thybaut, C.S.L. Narasimhan, J.F. Denayer, G.V. Baron, P.A. Jacobs, J.A. Martens, and G.B. Marin, Ind Eng Chem Res 44 (2005) 5159-5169.

[6] T.F. Degnan, and C.R. Kennedy, Aiche J 39 (1993) 607-614.

[7] M. Guisnet, Catal Today 218 (2013) 123-134.

[8] J.W. Thybaut, C.S.L. Narasimhan, G.B. Marin, J.F.M. Denayer, G.V. Baron, P.A. Jacobs, and J.A. Martens, Catal Lett 94 (2004) 81-88.

[9] G.G. Martens, G.B. Marin, J.A. Martens, P.A. Jacobs, and G.V. Baron, J Catal 195 (2000) 253-267.

[10] M.A. Baltanas, K.K. Vanraemdonck, G.F. Froment, and S.R. Mohedas, Ind Eng Chem Res 28 (1989) 899-910.

[11] J. Thybaut, and G.B. Marin, J Catal 308 (2013) 352-362.

[12] J.W. Thybaut, C.S.L. Narasimhan, and G.B. Marin, Catal Today 111 (2006) 94-102.

[13] C.S.L. Narasimhan, J.W. Thybaut, J.A. Martens, P.A. Jacobs, J.F. Denayer, and G.B. Marin, J Phys Chem B 110 (2006) 6750-6758.

[14] C.S.L. Narasimhan, J.W. Thybaut, J.F. Denayer, G.V. Baron, P.A. Jacobs, J.A. Martens, and G.B. Marin, Ind Eng Chem Res 46 (2007) 8710-8721.

[15] G.L. Aranovich, and M.D. Donohue, Colloid Surface A 187 (2001) 95-108.

[16] G.L. Aranovich, and M.D. Donohue, Langmuir 19 (2003) 2722-2735.

[17] F. Leroy, B. Rousseau, and A.H. Fuchs, Phys Chem Chem Phys 6 (2004) 775-783.

[18] H. Jobic, J Mol Catal a-Chem 158 (2000) 135-142.

[19] R.J. Madon, and E. Iglesia, J Mol Catal a-Chem 163 (2000) 189-204.

[20] C.S.L. Narasimhan, J.W. Thybaut, G.B. Marin, J.A. Martens, J.F. Denayer, and G.V. Baron, J Catal 218 (2003) 135-147.

[21] C.S.L. Narasimhan, J.W. Thybaut, G.B. Marin, P.A. Jacobs, J.A. Martens, J.F. Denayer, and G.V. Baron, J Catal 220 (2003) 399-413.

[22] C.S.L. Narasimhan, J.W. Thybaut, G.B. Marin, J.F. Denayer, G.V. Baron, J.A. Martens, and P.A. Jacobs, Chem Eng Sci 59 (2004) 4765-4772.

[23] I.R. Choudhury, J.W. Thybaut, P. Balasubramanian, J.F.M. Denayer, J.A. Martens, and G.B. Marin, Chem Eng Sci 65 (2010) 174-178.
[24] R.W. Hankinson, and G.H. Thomson, Aiche J 25 (1979) 653-663.
[25] S.W. Benson, F.R. Cruickshank, D.M. Golden, G.R. Haugen, H.E. Oneal, A.S. Rodgers, R. Shaw, and R. Walsh, Chemical Reviews 69 (1969) 279-324.
[26] J.F.M. Denayer, and G.V. Baron, Adsorption 3 (1997) 251-265.
[27] D. Peng, and D.B. Robinson, Ind Eng Chem Fund 15 (1976) 59-64.
[28] J.M. Moysan, M.J. Huron, H. Paradowski, and J. Vidal, Chem Eng Sci 38 (1983) 1085-1092.
[29] C. Reid, J.M. Prausnitz, B.E. Poling, The Properties of Gases and Liquids. McGraw-Hill International Editions, 1988, 742.